Pyramid wavefront sensing in the presence of thick spiders

Byron Engler[a], Miska Le Louarn[b], Christophe Vérinaud[b], Steve Weddell[a], and Richard Clare[a]

[a]Department of Electrical and Computer Engineering, Private Bag 4800, Christchurch, New Zealand

[b]European Southern Observatory, Karl-Schwarzschild Straße 2, Garching bei Muenchen, Germany

ABSTRACT

One of the challenges faced by the adaptive optics systems on extremely large telescopes, such as the European Extremely Large Telescope (EELT), is the pupil segmentation caused by the secondary mirror support structure (spider). We introduce a sensitivity metric to evaluate the sensitivity of the pyramid wavefront sensor to segment piston and propose a hybrid control method where both modulated and unmodulated pyramid wavefront sensor measurements are used. The modulated measurements correct the bulk of the atmospheric turbulence whilst the unmodulated measurements are used to correct the residual segment piston errors. Our hybrid approach provides a 5.6% improvement in Strehl under poor seeing (r_0 =10 cm) and 2.7% improvement under good seeing conditions (r_0 =20 cm).

Keywords: wavefront sensing, adaptive optics, pyramid wavefront sensor, EELT, petaling, segment piston

1. INTRODUCTION

There is a significant challenge in wavefront estimation for extremely large telescopes, such as the European Extremely Large Telescope,[1] which have large secondary mirror support structures. The secondary mirror support structure (spider) will be wide enough to obstruct entire rows and columns of wavefront sensor (WFS) sub-apertures (the spider is 1.58 sub-apertures wide) and will be larger than the expected r_0 at the telescope sites. This means that the atmospheric turbulence in each segment will be decorrelated. For the EELT, the spider structure has a 6-fold symmetry, resulting in six pupil segments (sometimes called islands, petals or fragments and to some extent, the low wind effect[2–5]) as shown in Fig. 1a.

A major challenge with the segmented pupil is during wavefront estimation using standard techniques, a piston error is introduced on each segment, as shown in Fig. 1b, which has a significant impact on the closed-loop Strehl and image quality within high contrast imaging systems. Others have proposed solutions to this problem such as slaving deformable mirror (DM) actuators on either side of the spider arm,[4] and using a two controller system where segment piston is controlled independently from all other modes.[2]

We start off by investigating the sensitivity of the pyramid wavefront sensor[6] to segment piston modes and the factors which affect the sensitivity. We find that reducing the amount of modulation on the pyramid has a significant increase in the sensitivity to segment piston, with the most sensitive case being an unmodulated pyramid. We introduce the idea of a hybrid adaptive optics (AO) loop, where wavefront measurements are taken from a modulated pyramid to sense and control the bulk of the atmospheric wavefront error. Interleaved with the modulated measurements are unmodulated measurements, which are used to sense and control only the segment piston modes. The output of the two controllers is combined to command a single DM.

We expand on previous work,[7] where we showed that there was an optimal illumination threshold for active sub-aperture selection. We noted that the number of active sub-apertures varied with rotation angle of the spider relative to the pyramid edges and the closed-loop Strehl varied with spider rotation. In this paper, we investigate the angle of the spider arms relative to the pyramid, for a simple case of a 1-arm spider, with a thickness of one sub-aperture, on an 8 m telescope.

Further author information: (Send correspondence to Byron Engler.)
E-mail: byron.engler@pg.canterbury.ac.nz

In this paper, we analyse how the modulation radius affects the sensitivity of the pyramid wavefront sensor to segment piston. We also propose a new hybrid modulated/unmodulated approach for controlling segment piston errors. In Section 2 we introduce a performance metric for the sensitivity of the pyramid wavefront sensor to segment piston. In Section 2.1, we outline our hybrid modulated/unmodulated wavefront sensing approach and describe the current implementation within Octopus. We show the simulation results in Section 3. In Section 4 we show that there is an optimal alignment between the spider arms and the pyramid edges. Finally draw conclusions and discuss future research in this area in Section 5.

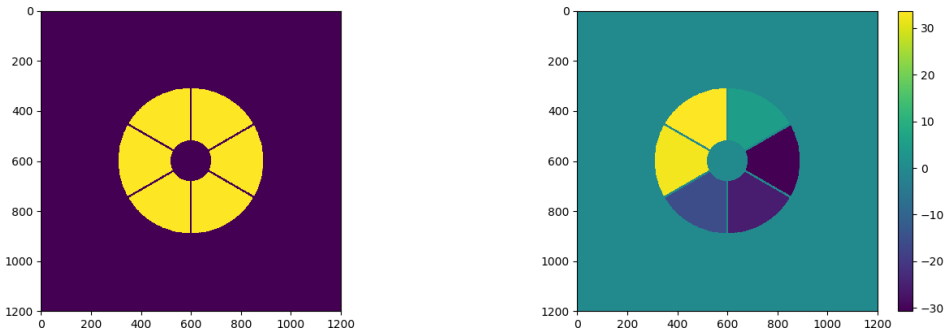

(a) (b)

Figure 1. (a) The pupil of a 37 m aperture and a 6-fold spider with 0.5 m thick arms. (b) A simulated example showing residual segment piston, in nanometers, after 1000 iterations in closed-loop.

2. METHODOLOGY

In order to investigate methods to control segment piston, we need a performance metric for the sensitivity of the pyramid WFS to the segment piston modes. We find the eigen values of an interaction matrix constructed from segment piston modes to be a good sensitivity metric. The higher the eigen value, the more sensitive the wavefront sensor is to the corresponding eigen mode. In simulation, using the pyramid WFS, an interaction matrix is created using only the six segment piston modes, as shown in Fig. 2. We then use singular value decomposition to find the eigen modes and associated eigen values of the interaction matrix.

$$H = USV^T, \tag{1}$$

where H is the interaction matrix, containing the WFS response to each segment piston mode, S is a diagonal matrix containing the singular values of the interaction matrix H, and U is the unitary matrix. The interaction matrix eigen modes are expressed as,

$$E_j(x, y) = \Sigma_{i=1}^{n} U(i, j) P_i(x, y), \tag{2}$$

where $E_j(x, y)$ is the j^{th} eigen mode and $P_i(x, y)$ is the i^{th} segment piston mode (in our case there are six segment piston modes). The eigen value associated with the j^{th} eigen mode is the j^{th} diagonal element of the the S matrix.

The eigen modes are shown in Fig. 3 in descending order of associated eigen value. To test the performance metric, the eigen modes and eigen values of a pyramid WFS interaction matrix, containing only the six piston modes, are calculated for different modulation radii. The results are plotted in Fig. 4 and show that reducing the modulation radius increases the sensitivity of the pyramid WFS to the segment piston modes. From the realisation that at zero modulation, the sensitivity to the segment piston modes significantly increases led to the development of a hybrid modulated/unmodulated method. This increased sensitivity to segment piston modes is also shown in closed-loop. Fig. 5 shows the residual segment piston in closed-loop with a modulated and unmodulated pyramid wavefront sensor, where each case has an initial segment piston waffle of 100 nm.

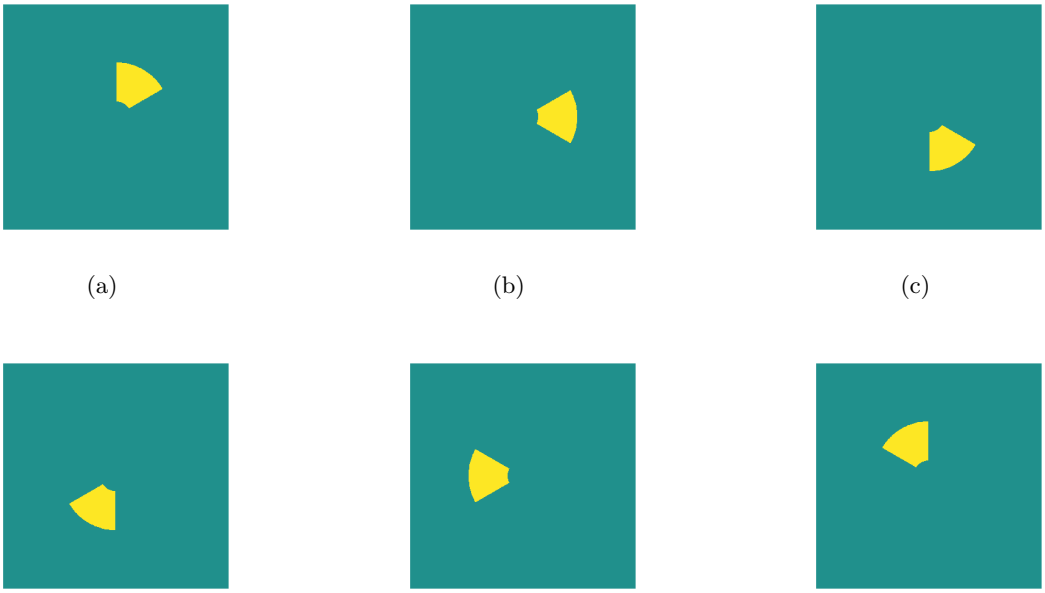

(a) (b) (c)

(d) (e) (f)

Figure 2. The six segment piston modes $P(x, y)$ for a 37 m segmented pupil. The spider arm width is 0.5 m.

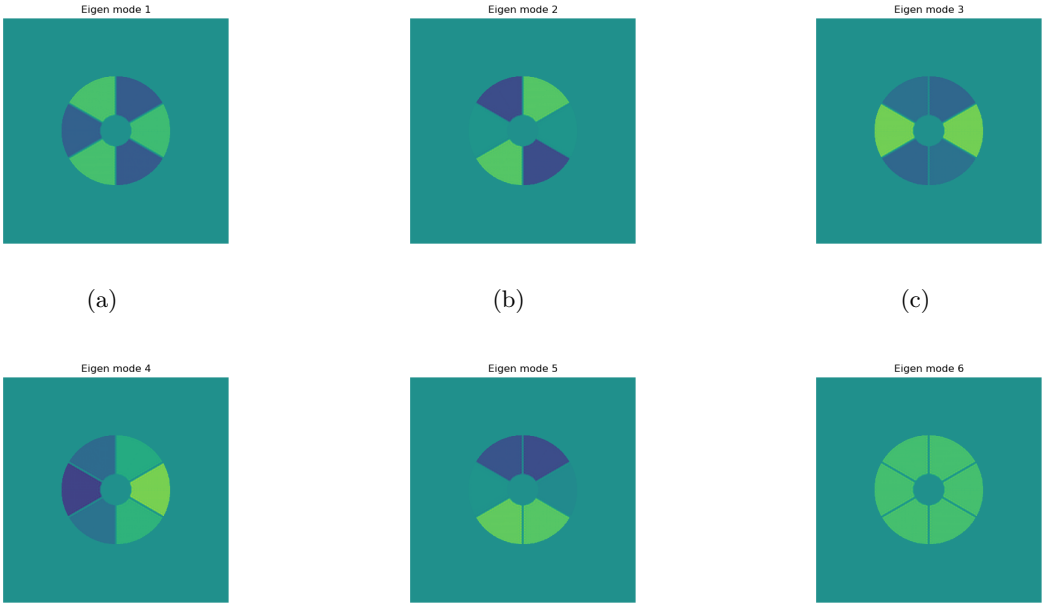

(a) (b) (c)

(d) (e) (f)

Figure 3. The six segment piston modes are used to generate an interaction matrix. Using singular value decomposition, the eigen modes and eigen values of the interaction matrix are found. Shown here are the eigen modes ordered from highest to lowest eigen value (from a-f).

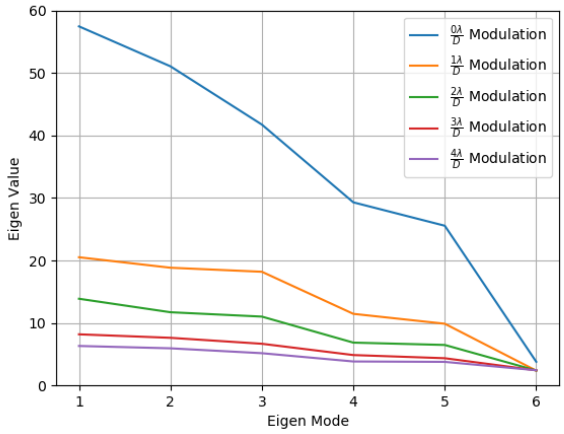

Figure 4. Using the eigen values of the associated eigen modes for the six segment piston modes as a sensitivity metric, we show that as the modulation radius of the pyramid wavefront sensor is reduced, the sensitivity of the segment piston modes increases. At zero modulation, the sensitivity is at its highest.

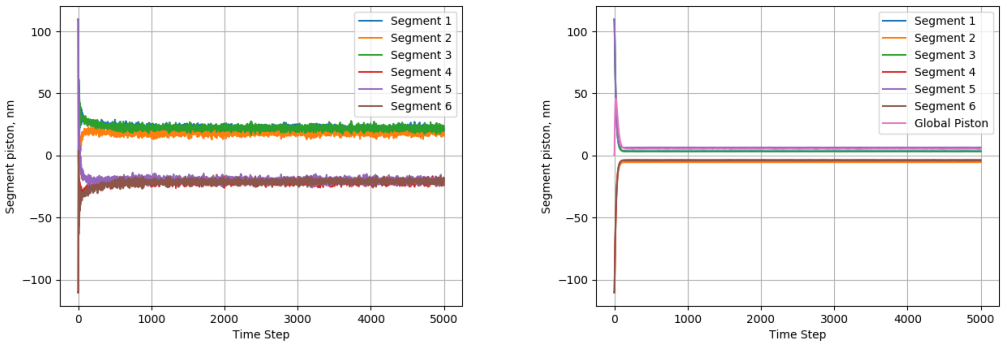

(a) (b)

Figure 5. To show that an unmodulated pyramid WFS has improved sensitivity to the segment piston modes, two cases were examined. For both cases, an interaction matrix is generated with only the six segment piston modes and a segment piston waffle is applied (eigen mode 1) with an amplitude of 100 nm. (a) The segment piston waffle corrected with a pyramid wavefront sensor with $\frac{4\lambda}{D}$ modulation. (b) The segment piston waffle corrected with an unmodulated pyramid wavefront sensor.

The hybrid modulated/unmodulated method uses a single pyramid wavefront sensor in two modes. A modulated mode $(\frac{4\lambda}{D})$[8] and an unmodulated mode. The modulated pyramid provides the required dynamic range to close the loop and control the majority of the atmospheric wavefront error, whilst the unmodulated pyramid's increased sensitivity to segment piston modes is used to correct any segment piston that arises. The AO loop is first closed with the modulated pyramid, and once the loop is closed and stable, the modulator is stopped and an unmodulated measurement is taken and then modulation resumes. The unmodulated measurements can be taken at a low rate as the temporal evolution of the segment piston modes is slow relative to the atmosphere, as shown if Fig. 6. The normalised cumulative power spectral density of the residual segment piston shows that 95% of the temporal evolution occurs at a rate at or below 100 Hz. The cumulative power spectral density is the cumulative integral of the power spectral density over the frequency axis. The integral over the entire spectral range will give a value of one.

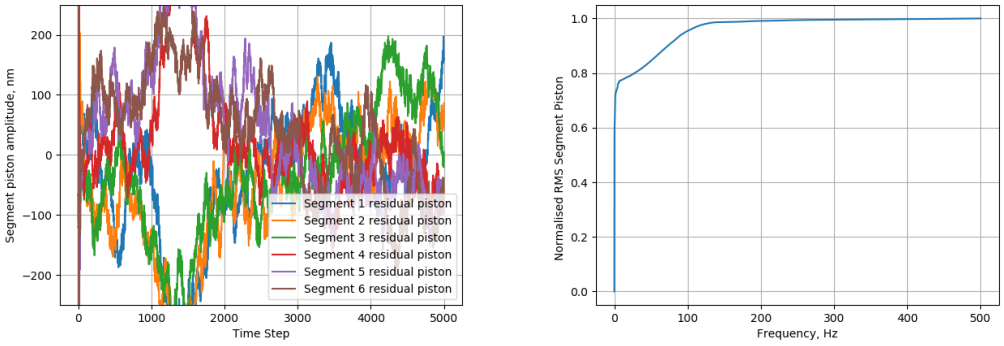

(a) (b)

Figure 6. For the hybrid modulated approach to work, we need to know how frequently we need to correct the residual segment piston error. (a) The residual segment piston error with an atmosphere with r_0 of 15 cm, using a modulated pyramid wavefront sensor and making no special effort to correct the segment piston errors. (b) The normalised cumulative power spectral density of (a).

Table 1. Simulation parameters used in this paper.

Parameter	Value
Fried parameter (r_0)	10 cm, 15 cm, 20 cm
Outer Scale (L_0)	25 m
Atmosphere	ESO 35 layer model
Telescope Diameter (D)	37 m
Frame Rate	1 kHz
Delay	2 Frames
WFS Wavelength (λ_W)	2200 nm
WFS Order	116 × 116 Subapertures
PSF Wavelength	2.2 µm
Modulation Width	$4\lambda_w/D$, $0\lambda_w/D$
Time Steps	1000
Spider Arms	6
Spider Arm Width	50 cm

2.1 Simulation Procedure

All the simulations are performed using the European Southern Observatory's Octopus simulation tool.[9] The important simulation parameters are listed in Tab. 1. As a proof of concept our hybrid modulated/unmodulated technique was implemented in Octopus as two separate simulation runs. First, a closed-loop simulation is done with a modulated pyramid wavefront sensor and a full interaction matrix (5190 modes). At each time-step, the atmospheric phase-screen, DM command and residual wavefront are saved. Secondly, a closed-loop simulation is done with an unmodulated pyramid wavefront sensor and an interaction matrix made up of only the six segment piston modes. At each iteration, the atmospheric phase-screen and DM commands from the modulated prism simulation are loaded (the unmodulated prism effectively sees the residual wavefront from the modulated simulation). Using the six segment piston mode interaction matrix, the DM command is calculated and summed with the modulated pyramids DM command. The resulting residual wavefront is free of both atmospheric and segment piston error. It should be noted that this is a pseudo closed-loop scenario as the final corrected wavefront is never presented to the modulated pyramid simulation. A block diagram of this process is shown in Fig. 7.

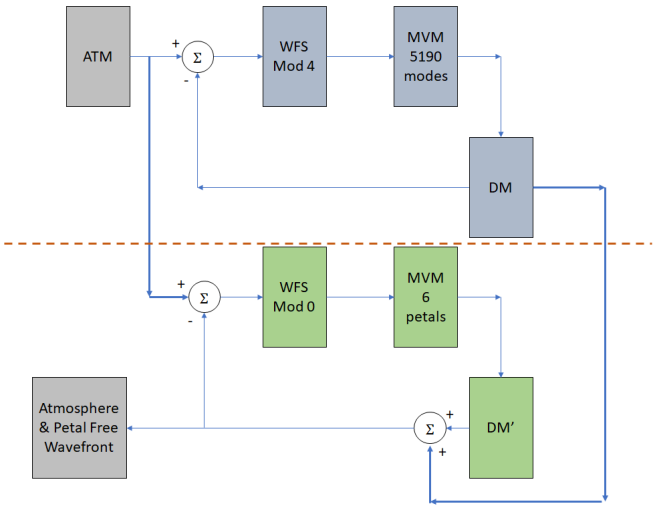

Figure 7. A block diagram of how our modulated/unmodulated approach is implemented in simulation. In simulation, this is broken into two separate simulation runs, a modulated pyramid (above dotted line) and an unmodulated pyramid(below dotted line). First, an atmospheric wavefront is sensed with a modulated pyramid WFS with a full interaction matrix (5190 modes), and at each time-step the DM commands are saved. During the second run (unmodulated), the same atmospheric wavefront is used but this time an unmodulated pyramid WFS with an interaction matrix of just the six petal modes. At each time step, the DM command generated by the unmodulated pyramid WFS and the corresponding DM command from the modulated WFS is summed and used to correct the wavefront.

3. SIMULATION RESULTS

Our hybrid modulated/unmodulated pyramid wavefront sensor approach is tested with different levels of atmospheric turbulence (r_0 of 10 cm, 15 cm and 20 cm) representing good, average and poor seeing conditions. The residual phase resulting from the modulated pyramid wavefront sensor path is analysed and the segment piston is measured. Then the unmodulated path is run and the resulting residual phase screens are again analysed and the segment piston measured. The segment piston over a single segment is plotted over time in Fig. 8, showing the amount of segment piston before and after using an unmodulated pyramid wavefront sensor to correct the segment piston. Our method significantly reduces segment piston, even in challenging seeing conditions.

As a measure of PSF quality, the Strehl ratio is computed using the residual phase-screens before and after the unmodulated prism is used for segment piston correction. The temporal evolution of the closed-loop Strehl is shown in Fig. 9. Even under poor atmospheric conditions, our hybrid modulated/unmodulated segment piston control method significantly improves the closed-loop Strehl by 5.6% (from 70.8% to 76.5%) and under the best atmospheric conditions tested, we show a 2.7% improvement in the closed-loop Strehl (from 89.5% to 92.3%).

4. POSITION OF SPIDER ARMS RELATIVE TO THE PYRAMID EDGES

For telescopes with thick spider arms, where they obstruct rows and columns of sub-apertures, such as the EELT, the number of active sub-apertures varies with the rotation of the spider. In a simplified test case, with an 8 m telescope and a 1-arm spider with a thickness of 20 cm, we found that the closed-loop Strehl varies with rotation of the spider relative the edges of the pyramid. For each rotation angle, the loop gain and regularisation is tuned for maximum closed-loop Strehl. Fig. 10 shows a 15% variation in closed-loop Strehl between an optimal alignment (0 and 90 degrees) when compared to the worst case (45 degrees) as well as the number of active sub-apertures. The variation in Strehl has a sinusoidal variation, whilst the number of sub-apertures has a more step-like response, this suggests that the Strehl variation is not related to the number of active sub-apertures.

For wavefront sensors that don't receive a derotated beam, the closed-loop performance of the AO system will depend on the orientation of the telescope. For instruments which account for field rotation, it will be important to get the optimal alignment of the pyramid and spider to obtain the highest performance of the AO system.

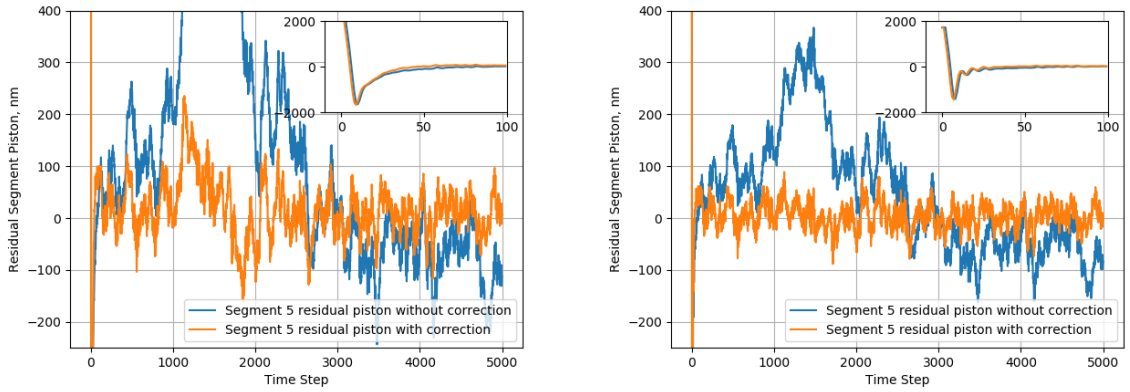

(a)

(b)

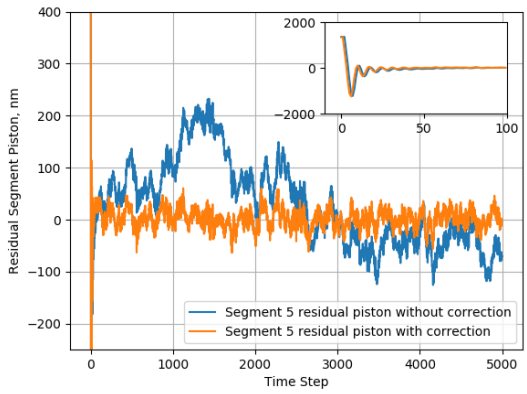

(c)

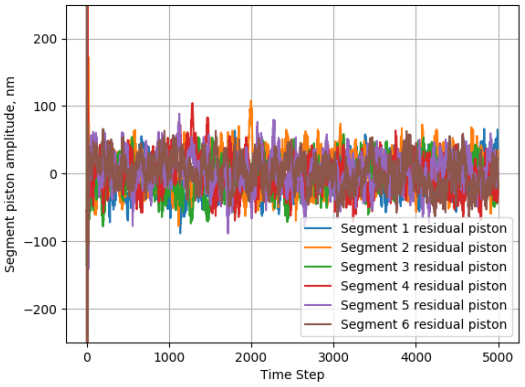

(d)

Figure 8. Temporal evolution of the residual segment piston, without (blue) and with (orange) our hybrid modulated/unmodulated method for segment piston control, where the atmosphere has an r_0 of 10cm (a), 15cm (b) and 20cm (c). The inset plots show the first 100 time steps, where a large segment piston is quickly corrected. We show the residual segment piston, for each segment, after our hybrid modulated/unmodulated control method for an atmosphere with an r_0 of 20cm (d).

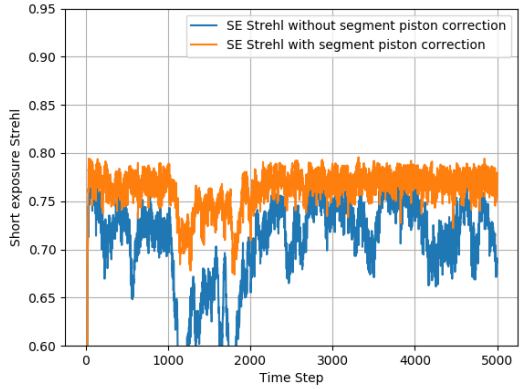

(a)

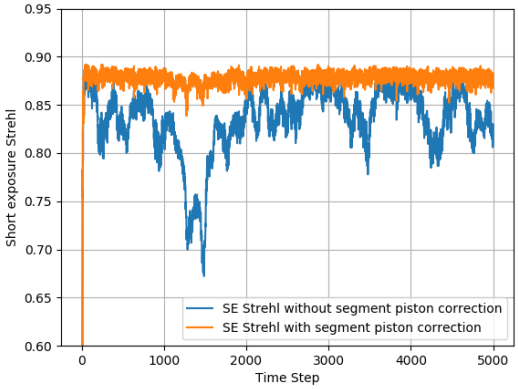

(b)

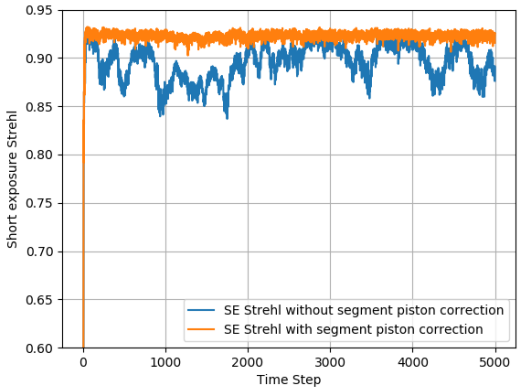

(c)

Figure 9. The short exposure, closed-loop K-band Strehl for a pyramid WFS with a modulation of $\frac{4\lambda}{D}$ (blue), and for our hybrid modulated/unmodulated method (orange). The performance is evaluated for an r_0 of 10 cm (a), 15 cm (b) and 20 cm (c).

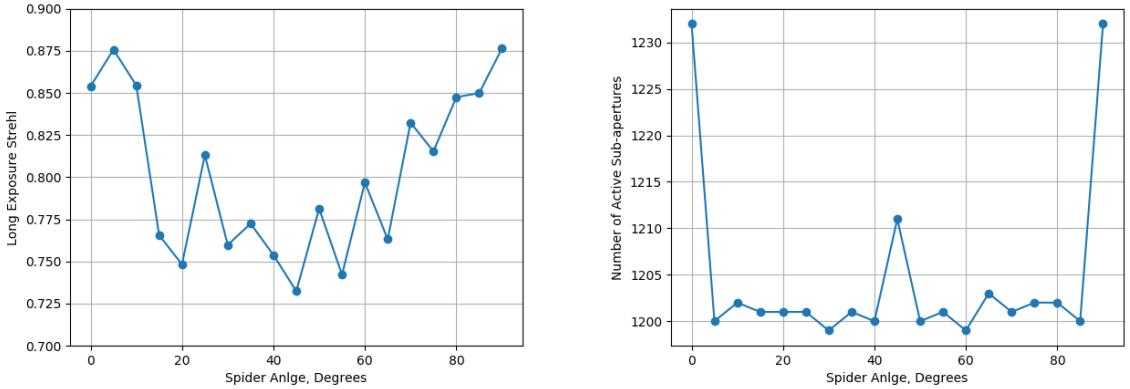

(a) (b)

Figure 10. A simplified test case with an 8 m diameter mirror and a 1-arm spider. The spider is rotated relative to the pyramid, at each rotation step a full closed-loop simulation is performed. (a) The closed-loop Strehl varies with spider rotation, with optimal Strehl when the spider arm and pyramid edge are parallel (0 and 90 degrees). (b) The number of active sub-apertures used in wavefront estimation also varies with spider rotation, because of the constant illumination threshold.

5. CONCLUSION

We have shown that using an unmodulated pyramid wavefront sensor can significantly reduce the segment piston problems faced by large diameter telescopes with thick spiders. Our simulation results presented here demonstrate the concept, however they are not truly closed-loop. The next step is to have a fully closed-loop system, with two controllers running at different rates. This would show that our method could be useful in a functional AO system. We also expect to be able to further increase the sensitivity of the unmodulated pyramid wavefront sensor to segment piston modes by filtering the measurements used. Hutterer *et al.*[2] show that the signal measured from a pyramid wavefront sensor presented with a segment piston is concentrated around the spider arms of the actuated segment. Using this response, the measurements could be further filtered to improve the signal-to-noise ratio of the segment piston modes.

We have shown that using the eigen values of the six segment piston modes is a useful sensitivity metric for the pyramid wavefront sensor to segment piston. Using this sensitivity metric, we show that an unmodulated pyramid provides a significant increase in sensitivity to segment piston modes. Using the increased sensitivity of the unmodulated pyramid, we propose a hybrid wavefront sensor approach, where two control-loops are implemented. One control-loop uses a full (5180 modes) interaction matrix and a modulated pyramid wavefront sensor sampled at 1kHz. The second loop uses an interaction matrix of only the six segment piston modes and an unmodulated pyramid wavefront sensor. The unmodulated measurements are interleaved with the modulated measurements. We propose that the unmodulated loop could be run at approximately 100Hz to be effective. We have shown that the hybrid approach shows promise, in a pseudo closed-loop scenario, reducing the segment piston error from 100 nm to 25 nm for an r_0 of 20 cm.

The alignment of the spider with the pyramid edges has a notable impact on closed-loop Strehl. There is a variation in closed-loop Strehl of approximately 15% when the spider arm is optimally aligned with the pyramid (0 and 90 degrees) when compared to the worst case alignment of 45 degrees. In the future we plan to perform this same analysis with different geometry pyramids (3-sided and 6-sided) and spider designs.

REFERENCES

[1] Cayrel, M., "E-ELT optomechanics: overview," in [*Ground-based and Airborne Telescopes IV*], International Society for Optics and Photonics, SPIE (2012).

[2] Hutterer, V., Shatokhina, I., Obereder, A., and Ramlau, R., "Advanced wavefront reconstruction methods for segmented Extremely Large Telescope pupils using pyramid sensors," *Journal of Astronomical Telescopes, Instruments, and Systems* (2018).

[3] Bonnefond, S., Tallon, M., Le Louarn, M., and Madec, P.-Y., "Wavefront reconstruction with pupil fragmentation: study of a simple case," in [*Adaptive Optics Systems V*], International Society for Optics and Photonics, SPIE (2016).

[4] Schwartz, N., Sauvage, J.-F., Correia, C., Neichel, B., Fusco, T., Quiros-Pacheco, F., Dohlen, K., Hadi, K. E., Agapito, G., Thatte, N., and Clarke, F., "Analysis and mitigation of pupil discontinuities on adaptive optics performance," in [*Adaptive Optics Systems VI*], International Society for Optics and Photonics, SPIE (2018).

[5] Marchetti, E., Close, L. M., Vran, J.-P., Sauvage, J.-F., Fusco, T., Lamb, M., Girard, J., Brinkmann, M., Guesalaga, A., Wizinowich, P., O'Neal, J., N'Diaye, M., Vigan, A., Mouillet, D., Beuzit, J.-L., Kasper, M., Le Louarn, M., Milli, J., Dohlen, K., Neichel, B., Bourget, P., Haguenauer, P., and Mawet, D., "Tackling down the low wind effect on sphere instrument," (2016).

[6] Ragazzoni, R., "Pupil plane wavefront sensing with an oscillating prism," *Journal of Modern Optics* (1996).

[7] Engler, B., Weddell, S., Le Louarn, M., and Clare, R., "Effects of the telescope spider on extreme adaptive optics systems with pyramid wavefront sensors ," in [*Adaptive Optics Systems VI*], International Society for Optics and Photonics, SPIE (2018).

[8] Clare, R. and Le Louarn, M., "Numerical simulations of an extreme AO system for an ELT," (2011).

[9] Le Louarn, M., Verinaud, C., Korkiakoski, V., and Fedrigo, E., "Parallel simulation tools for AO on ELTs," in [*Advancements in Adaptive Optics*], International Society for Optics and Photonics, SPIE (2004).